MIT Libraries | DSpace@MIT

MIT Open Access Articles

Mechanism and Control of Continuous-State Coupled Elastic Actuation

The MIT Faculty has made this article openly available. ***Please share*** how this access benefits you. Your story matters.

Citation: Huang, Tzu-Hao, Han-Pang Huang, and Jiun-Yih Kuan. "Mechanism and Control of Continuous-State Coupled Elastic Actuation." J Intell Robot Syst 74, no. 3–4 (September 22, 2013): 571–587.

As Published: http://dx.doi.org/10.1007/s10846-013-9937-0

Publisher: Springer Netherlands

Persistent URL: http://hdl.handle.net/1721.1/103619

Version: Author's final manuscript: final author's manuscript post peer review, without publisher's formatting or copy editing

Terms of Use: Article is made available in accordance with the publisher's policy and may be subject to US copyright law. Please refer to the publisher's site for terms of use.

Massachusetts Institute of Technology

J Intell Robot Syst
DOI 10.1007/s10846-013-9875-x

Mechanism and Control of Continuous-State Coupled Elastic Actuation

Tzu-Hao Huang · Han-Pang Huang · Jiun-Yih Kuan

Received: 21 February 2013 / Accepted: 21 August 2013
© Springer Science+Business Media Dordrecht 2013

Abstract Focusing on the physical interaction between people and machines within safety constraints in versatile situations, this paper proposes a new, efficient, coupled elastic actuation (CEA) to provide future human-machine systems with an intrinsically programmable stiffness capacity to shape the output force corresponding to the deviation between human motions and the set positions of the system. As a possible CEA system, a prototype of a two degrees of freedom (2-DOF) continuous-state coupled elastic actuator (CCEA) is designed to provide a compromise between performance and safety. Using a pair of antagonistic four-bar linkages, the inherent stiffness of the system can be adjusted dynamically. In addition, the optimal control in a simple various stiffness model is used to illustrate how to find the optimal stiffness and force trajectories. Using the optimal control results, the shortest distance control is proposed to control the stiffness and force trajectory of the CCEA. Compared to state-of-the-art variable stiffness actuators, the CCEA system is unique in that it can achieve near-zero mechanical stiffness efficiently and the shortest distance control provides an easy way to control various stiffness mechanisms. Finally, a CCEA exoskeleton is built for elbow rehabilitation. Simulations and experiments are conducted to show the desired properties of the proposed CCEA system and the performance of the shortest distance control.

Keywords Variable stiffness mechanism · Variable stiffness control · Optimal control · Continuous-state coupled elastic actuation

1 Introduction

In modern robotics, physical human-robot interaction (pHRI) is the current focus. Considering the trade-off between safety and performance, robots are designed to be intrinsically safe for human-robot interaction [1, 2]. In particular, robots, which provide services during labor shortages or assist the disabled with daily activities due to longevity problems, are the major focuses.

To achieve safe and efficient manipulation, the designs should consider all mechanisms, electronics, control, and software architectures. Although

Q1

T.-H. Huang (✉) · H.-P. Huang
Department of Mechanical Engineering,
National Taiwan University, Taipei, Taiwan
e-mail: d95522013@ntu.edu.tw

H.-P. Huang
e-mail: hanpang@ntu.edu.tw

J.-Y. Kuan
Department of Mechanical Engineering,
Massachusetts Institute of Technology,
Cambridge, USA

modifying the controllers of rigid robots with additional sensors has demonstrated effectiveness in safe manipulation [3–5], some performance limitations, however, are due to the imperfect mechanical design [1, 6, 7]. In particular, passive compliance mechanisms that reduce transmission stiffness are regarded as one of the most promising designs.

Recently, several safe and efficient robot actuation techniques have been proposed, such as series elastic actuators (SEAs) [6–13], programmed impedance actuators [14, 15], and variable stiffness actuators [15–22]. In all these designs, a critical feature is the stiffness of the series elastic component, which dominates the bandwidth and the payload capacity of the overall system, and therefore the safety level in the pHRI field. Most of the works cited are designed with a constant stiffness. Although these mechanisms possess intrinsic safety, the control performance is sacrificed because of the necessary stability for various users and tasks. Distinct from designed actuators with constant stiffness, the human muscular system possesses inherent advantages in its adaptive, elastic nature, resulting in minimized work and peak power [23–25], which, in the actuator aspect, reduces the required weight of the actuator [22, 26–28]. Therefore, variable stiffness actuation plays an important role in the next generation of robotics.

To realize the stiffness adaptively, a popular approach is to implement two opposing actuators of similar capacity in series with variable stiffness elements. By utilizing two actuators, the magnitude of the output is determined by the common motion of the actuators, whereas the stiffness can be changed according to differential motion [17, 20, 29]. Due to the antagonistic setting, the actuators are required to consistently exert torque on the output link to maintain stiffness, which results in a large waste of energy.

To design a more practical actuation that can be used adaptively in rehabilitative and assistive motions, a continuous-state coupled elastic actuator (CCEA) is introduced. The main contribution of this work is the realization of the CCEA mechanism, the formulation of the optimal control problem for general variable stiffness control, and the shortest distance optimization method for the CCEA or any type of variable stiffness mechanism.

The design concept and mechanical properties of the proposed mechanism are addressed in Section 2. A possible optimal stiffness and equilibrium position control in a simple various stiffness mode is proposed in Section 3. The stiffness and force control of the CCEA by the shortest distance control method is proposed in Section 4. The mechanical property of the CCEA, the simulation results, and the experimental results are derived and explained in Section 5. Simulations and experiments are also addressed. Finally, the conclusion follows.

2 Design of a Continuous-State Elastic Actuator

The purpose of the continuous-state elastic actuator (CEA) is to generate the reaction force profile relating the deviation of the output link to the set position of the system by using a set of components with different elastic properties. As shown in Fig. 1, compared with typical compliant actuators, the coupled elastic elements and stiffness-adjusting mechanisms do not move with the output link. Therefore, the inertia of the output can be kept as small as possible, and the operation range of the output position could theoretically be unlimited. Although the output is not directly connected to the input via the coupled elastic elements, it still possesses a similar effect as the typical SEA, in which the output force is zero, if no reaction force is provided by the elastic elements. Moreover, the power input is always protected, since it is virtually decoupled from the output link.

In this paper, a new CCEA system is constructed using a pair of antagonistic four-bar linkages. The CCEA, as one of the CEAs, can dynamically adjust the stiffness of the system by tuning the equilibrium position of the preload. The detailed working principles and the design are addressed in the following section.

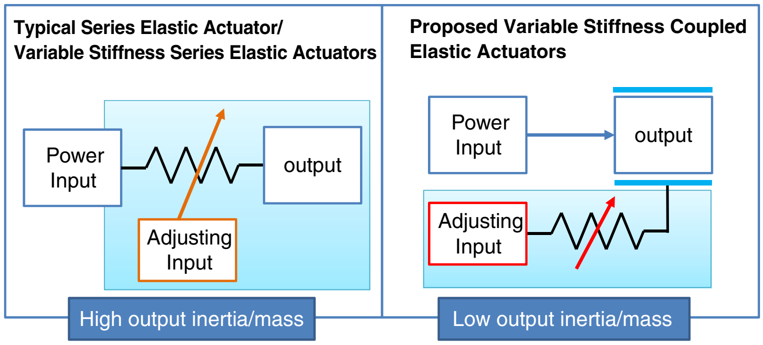

Fig. 1 Comparison of topology of the proposed general variable stiffness coupled elastic actuators approach and typical series elastic/variable elastic actuators

2.1 CCEA Design Concept - Single Four-Bar Linkage

First, we consider a single four-bar linkage with an extensional linear spring configured as in Fig. 2, where the mass of the stiffness adjuster is M_{ac}, the mass of the output carriage is M_{ca}, the stiffness adjusting force is F_{ac}, the displacement of the stiffness adjuster is X_{ac}, the displacement of the output carriage is X_{ca}, and the external load force is F_1. The length of the linkages, R_1 and R_2, are set to be R for convenience. Thus, the transmission angle of the four-bar linkage $\beta \in (0, 2\pi)$ can be defined as follows:

Q2

$$\beta = \cos^{-1}\left(\frac{X}{2R}\right), \tag{1}$$

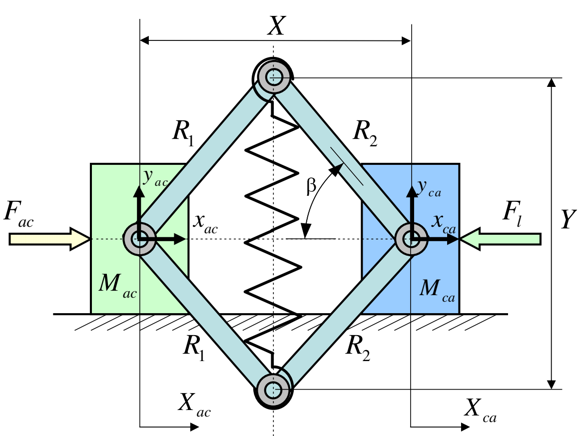

Fig. 2 Topology of the proposed continuous-state

where the displacement between the stiffness adjuster and the output mass is

$$X = 2R - X_{ac} + X_{ca}, \tag{2}$$

and the potential energy stored in the spring of the CCEA can be formulated as

$$P(X) = \frac{1}{2}K_t \Delta Y^2 = \frac{1}{2}K_t (Y - Y_0)^2, \tag{3}$$

where $Y_0(X_0) = \sqrt{4R^2 - X_0^2}$ is the non-stressed length, and K_t is the stiffness constant of the linear spring. Due to the deflection ΔY of the linear spring, the restored force on the output link, which is the function of the geometry, can be written as follows:

$$F(X) = \frac{\partial P}{\partial X} = -K_t \cdot X\left(1 - \sqrt{\frac{4R^2 - X_0^2}{4R^2 - X_2}}\right). \tag{4}$$

Thus, the stiffness is:

$$\begin{aligned} K(X) &= \frac{\partial^2 P}{\partial X^2} = \frac{\partial F}{\partial X} \\ &= -K_t\Big[1 - \left(4R^2 - X^2\right)^{-\frac{1}{2}}\left(4R^2 - X_0^2\right)^{\frac{1}{2}} \\ &\quad + K_t X^2\left(4R^2 - X^2\right)^{-\frac{3}{2}}\left(4R^2 - X_0^2\right)^{\frac{1}{2}}\Big] \\ &= -K_t\Big[1 - \left(4R^2 - X^2\right)^{-\frac{1}{2}}\left(4R^2 - X_0^2\right)^{\frac{1}{2}} \\ &\quad + X^2\left(4R^2 - X^2\right)^{-\frac{3}{2}}\left(4R^2 - X_0^2\right)^{\frac{1}{2}}\Big] \end{aligned} \tag{5}$$

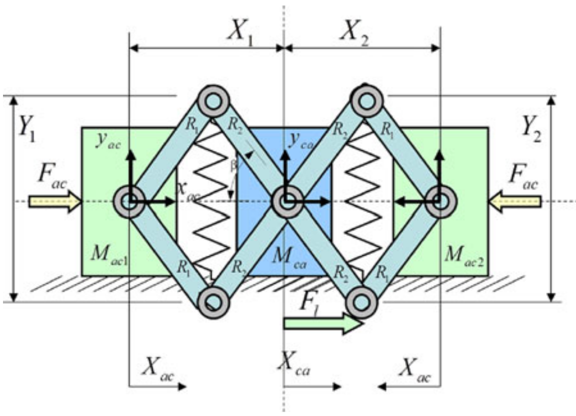

Fig. 3 Topology of the antagonistic coupled elastic actuation

2.2 CCEA Design Concept - Antagonistic Four-Bar Linkages

Using the model derived above, the intrinsic properties of a pair of antagonistically identical four-bar linkages with two extensional linear springs are shown in Fig. 3, in which the total deflection of the system X_{ca} is defined such that

$$X_1 = 2R - X_{ac} + X_{ca}; \quad X_2 = 2R - X_{ac} - X_{ca}$$
$$R = 12.2mm; \ X_0 = 14mm; \quad K_t = 62\left(N/mm\right) \tag{6}$$

$$\begin{cases} P_{CCEA}\left(X_{ac}, X_{ca}\right) = P_1\left(X_1\right) + P_2\left(X_2\right) \\ F_{CCEA}\left(X_{ac}, X_{ca}\right) = F_1\left(X_1\right) - F_2\left(X_2\right) \\ K_{CCEA}\left(X_{ac}, X_{ca}\right) = K_1\left(X_1\right) + K_2\left(X_2\right) \end{cases} . \tag{7}$$

2.3 Practical CCEA Design and Working Principle

Based on the proposed design, the resultant CCEA is shown in Fig. 4. In this design, a worm drives a worm gear through a pair of four-bar linkages with linear extensional springs and a set of coupled parallel soft linear compression springs, which initially restrain the movement of the worm shaft in its axial direction; two additional motors

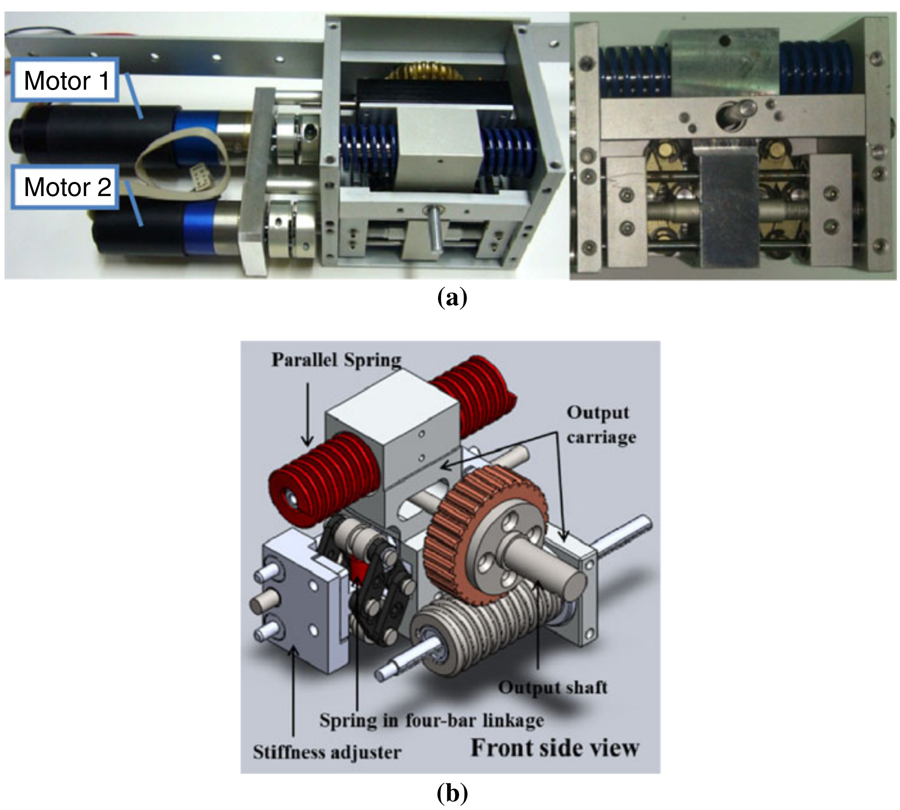

Fig. 4 Continuous-state coupled elastic actuator. **a** The fabricated CCEA. **b** A three-dimensional view of the CCEA

control the output force and the stiffness of the system.

Figure 5a shows how the stiffness can be adjusted by Motor 2. The rotation of Motor 2 drives a both-end-thread screw along which two movable blocks and stiffness adjusters are conveyed simultaneously. Then the associated transmission angles of the four bar linkages change. Figure 5b shows how the force can be generated by Motor 1. The rotation of Motor 1 drives the worm that drives the worm gear directly coupled with the output linkage. Figure 5c shows the mechanism of the variable stiffness actuation. When external force is exerted on the output linkage, the worm gear moves, and the spring compresses on one side and lengthens on the other side. Finally, Table 1 shows the specification of the CCEA mechanism.

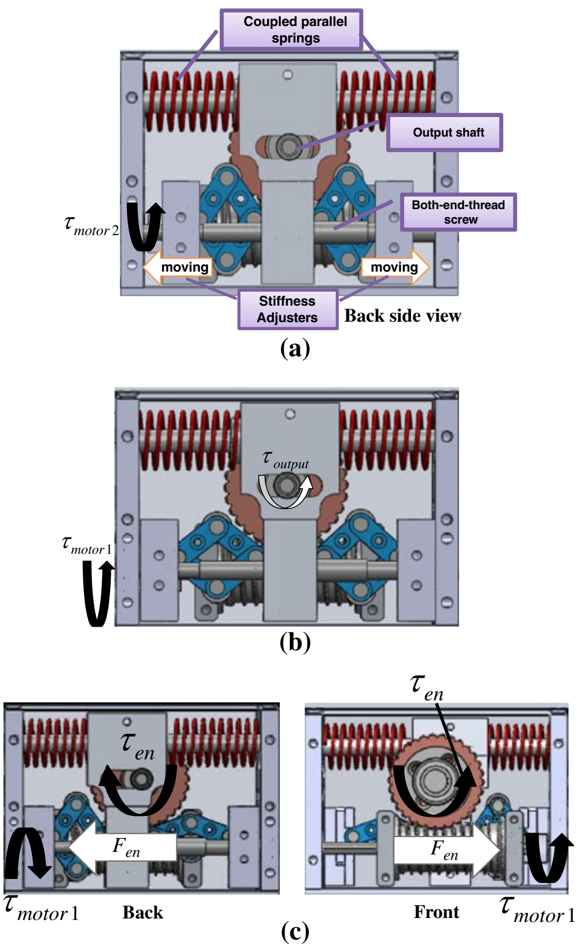

Fig. 5 Stiffness adjustment process and continuous-state coupled elastic actuation mechanism. **a** Motor 2 drives the stiffness adjusters that carry a pair of four-bar linkage. **b** Motor 1 drives the output shaft via a worm and gear pair. Output torque will be generated only when there is environment torque on the output link. **c** Load torque on the output shaft moves the worm, and shortens one hand side springs and lengthens the other hand side springs

Table 1 Specifications of the CCEA actuator

Weight (include the motor)	800 g
Length*Width*Height	$60 \times 600 \times 74$ mm^3
Reduction Ratio of Input to Output	1:30
Reduction Ratio of a Gear to a Pinion	1:1
Rated Output Torque	13 Nm
Rated Output Speed	86 deg/sec
Base Soft / Hard Spring Stiffness	62 / 171 Nm/mm
Max. Output Link Deflection	±72°
Stroke of the Stiffness Adjuster	12 mm

*The input motor used in this design is Faulhaber DC-micromotor 2657G024CR with a 26A gearhead that has a 1:13 reduction ratio.

3 Optimal Stiffness Control in a Simple Model of Variable Stiffness Actuation

To control the stiffness and the output force of this two degrees of freedom (2-DOF) CCEA, we adopt optimal control, which is used widely in problems of mechanisms [2, 4]. Because the influence on the stiffness of the two motors is coupled, the nonlinear system is too complex for conventional optimal control. Therefore, the CCEA model is simplified as the decoupled model, in which only one of the motors can control the stiffness. This simple variable stiffness model is modeled as an ideal variable stiffness actuation, so the stiffness and the equilibrium position can be controlled directly and independently. Although the nominal model is different from the real CCEA model, the nominal model simplifies the design of the stiffness and the output force. Because the CCEA mechanism is mainly composed of a worm and a worm gear, Motor 1 and Motor 2 are modeled as a non-back drivable system shown in Fig. 6. The mass, damper, and force of Motor 1 are m_1, B_1, and u_1. The mass, damper, and force of Motor 2 are m_2, B_2, and u_2. The displacements of

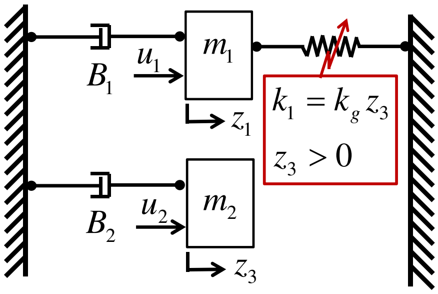

Q4 **Fig. 6** The CCEA can be modeled as this simplified model with two motors. The mass, damper, and force of Motor 1 are m_1, B_1, and u_1. The mass, damper, and force of Motor 2 are m_2, B_2, and u_2. The displacements of Motor 1 and Motor 2 are z_1 and z_2. The stiffness of the spring in the four-bar linkage is k_g. Motor 1 is used to actuate the output link, and Motor 2 is used to change the stiffness (k_1) of the CCEA

Motor 1 and Motor 2 are z_1 and z_2. The stiffness of the spring in the four-bar linkage is k_g. Motor 1 is used to actuate the output link, and Motor 2 is used to change the stiffness (k_1) of the CCEA.

With suitable variable stiffness, the energy efficiency and the dynamic range of the actuation can be improved [30]. Therefore, the requirement for the size and the weight of the actuator can be reduced, and the CCEA system can be more compact and competent. As in the introduction, the muscular system has excellent adaptive nonlinearity originating from the variable stiffness mechanism of muscles that can minimize the work and peak power in various tasks [23–28]. In this paper, we adopt this idea of minimizing the work and peak power in the actuator design [28, 31]. However, the other variable stiffness optimization methods consider the cost function regarding the control input, kinetic energy, and potential energy [32, 33]. To investigate the effect of the control input, kinetic energy, and the potential energy on the system, three different cost functions are chosen based on the following definition of optimality.

Definition of Optimality

The stiffness and the equilibrium position are optimal if

1. the energy of the cost function is minimized,
2. the total deflection of Motor 1 and Motor 2 are the least.

Since Motor 1 controls the equilibrium position, and Motor 2 controls the stiffness, the second requirement is more than a realistic limitation, which limits the stroke of Motor 1 and Motor 2. For instance, too soft stiffness implies a large deflection of Motor 1, which cannot be achieved in real use.

According to the definition of optimality, the cost function is chosen as shown, where J_0 is chosen as the $l2$-norm of the control input, the displacement, the velocity, and the tracking error, J_1 is the $l2$-norm of the control input, the displacement, and the tracking error, and J_2 is the $l2$-norm of the displacement and the tracking error. The parameters are defined as follows.

z_1 : Displacement of motor 1
z_3 : Displacement of motor 2
u_1 : Control input of equilibrium point
Z_1 : Control input of adjusted stiffness
Output Force : $y = k_1 z_1 = (k_g z_3) z_1$ k_g is set as 1
Tracking Force Trajectory : $r(t) = \sin(2\pi t)$, $t = 0 \sim 1$ Q5

The cost functions are:

$$\begin{cases} \min\ \mathrm{J}_0 = \displaystyle\int_0^T \mathbf{z}(t)^T \mathbf{z}(t) + \mathbf{u}(t)^T \mathbf{u}(t) + 100 * \left(k_g z_1 z_3 - r(t)\right)^2 dt \\ \min\ \mathrm{J}_1 = \displaystyle\int_0^T \mathbf{z}(t)^T \mathbf{R}\mathbf{z}(t) + \mathbf{u}(t)^T \mathbf{u}(t) + 100 * \left(k_g z_1 z_3 - r(t)\right)^2 dt \\ \min\ \mathrm{J}_2 = \displaystyle\int_0^T \mathbf{z}(t)^T \mathbf{R}\mathbf{z}(t) + 100 * \left(k_g z_1 z_3 - r(t)\right)^2 dt \end{cases} \tag{8}$$

$\mathbf{z}(t) = [z_1(t)\ z_2(t)\ z_3(t)\ z_4(t)]^T$; $\mathbf{R} = diag([1\ 0\ 1\ 0])$; $\mathbf{u}(t) = [u_1(t)\ u_2(t)]^T$ subject to

$$\begin{cases} \dot{z}_1 = z_2 \\ \dot{z}_2 = -\dfrac{B_1}{m_1} z_2 + \dfrac{1}{m_1} u_1 \\ \dot{z}_3 = z_4 \\ \dot{z}_4 = -\dfrac{B_2}{m_2} z_4 + \dfrac{1}{m_2} u_2 \\ z_3 > 0 \end{cases} \tag{9}$$

Solving non-quadratic optimal control with state inequality and constrained equality is not easy. To solve the optimization, control vector parameterization (CVP) is considered. Control vector parameterization known as the direct sequential method is a direct optimization method for solving optimal control problems. The basic idea of direct optimization methods is to discretize the control problem in the time domain and states, and then apply nonlinear programming (NLP) techniques to the resulting finite-dimensional optimization problem. This method is easy to implement, but the computation increases as the discretization becomes finer. Although it is impossible for real-time optimal control, in our study, CVP is mainly used to illustrate the method of adjusting the stiffness and the output force of the variable stiffness mechanism. Together with the shortest distance algorithm proposed in Section 4, the real-time variable stiffness control is possible with pre-computed CVP. In this paper, the CVP program is based on the MATLAB library, DOTcvp (Dynamic Optimization Toolbox with Control Vector Parameterization) [34]. The method breaks the control input into piecewise vectors, and each piecewise vector is an approximation of the real optimal control policy, such as constant, linear, or polynomial approximation. With the chosen sensitivity coefficients, which are the partial derivation of state variables regarding decision variables, the problem can be solved by using a general nonlinear programming solver. Here, we chose the nonlinear optimization solver FMINCON [35] in MATLAB, which uses sequential quadratic programming (SQP) to find the minimum of the constrained differentiable nonlinear multivariable function. Owing to the curse of dimensionality, the computational burden and the memory requirement of CVP increase exponentially with the size of the problem. However, for the size of our problem, it can still be solved in finite time.

4 Force and Stiffness Control in CCEA with the Shortest Distance Algorithm

In Section 3, optimal control for the simple variable stiffness model is discussed. However, the method for controlling the stiffness and force of the CCEA is still not clear. The assumptions for controlling the variable stiffness actuation imply that one of the best ways to control the CCEA is choose the shortest distance from the initial position to the end position, because the shortest distance during each sample period is similar to minimize the velocity term of variable stiffness actuation. Through the simple algorithm shown in Table 2, the complex CCEA optimal problem can be relaxed and approximated by the proposed

Table 2 The main procedure of the shortest distance control method for force and stiffness control in CCEA

Q3

Set an initial value in Point $P(0)$	
For	$k=0, \ldots, m-1$. m is the number of total trajectory points.
Step 1	From force lookup table $F_{\text{lookup\_table}}(X_{ac}, X_{ca})$,
	search those points $P_i = (X_{ac}, X_{ca})$ satisfy that the
	force of those points are near next force command $r(k+1)$.
	Find $\lvert F_{\text{lookup\_table}}(P_i) - r(k+1)\rvert < \delta$, $\delta = 0.01$
Step 2	Find the point $P^* = \left(X^*_{ac}, X^*_{ca}\right)$ which has the minimum
	cost $J^*_{sd} = \lVert P(k) - P^* \rVert_2$
Step 3	$P(k+1) = P^*_i$
End	

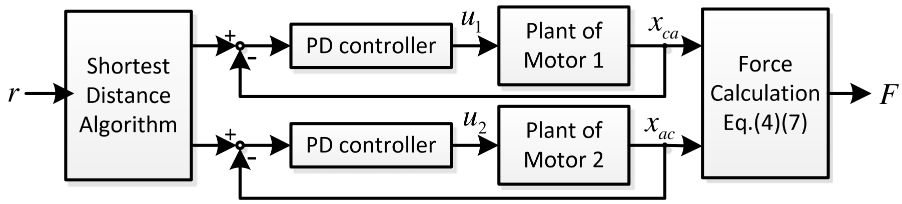

Fig. 7 The control flow of the CCEA torque control

shortest distance. In this method, the distance of Motor 1 and Motor 2 from the current position to the next position is calculated, and the value is used as the main objective function to minimize. The cost function for CCEA force control is the shortest distance in the 2-norm space [36]. d_1 is the distance from the current displacement to the next displacement of X_{ac}. d_2 is the distance

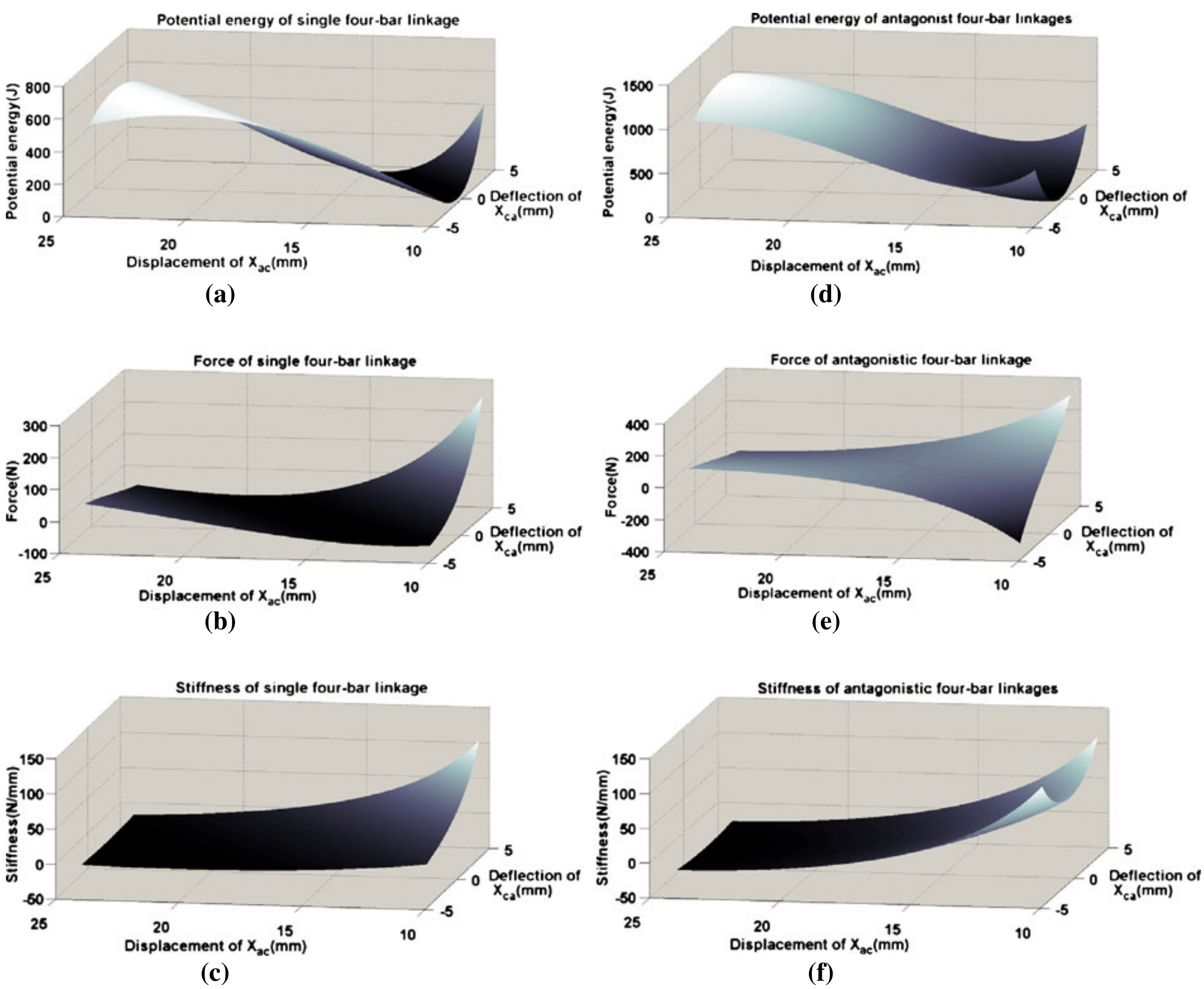

Fig. 8 Properties of the designed CCEA system. **a** Potential energy of single four-bar linkage. **b** Force of single four-bar linkage. **c** Stiffness of single four-bar linkage. **d** Potential energy of antagonist four-bar linkages. **e** Force of antagonist four-bar linkages. **f** Stiffness of antagonist four-bar linkages

from the current deflection to the next deflection of X_{ca}.

$$J_{sd} = \sqrt{d_1^2 + d_2^2} \tag{10}$$

The parameters for CCEA force control are defined as follows.

$r(k)$: the current force command
$r(k+1)$: the next force command
$P(k)$: the current deflection and displacement of motors
$P(k+1)$: the next deflection and displacement of motors
P_i : those points which force are near $r(k+1)$
P^* : the optimal point of P_i
$F_{\text{lookup\_table}}(X_{ac}, X_{ca})$: The force lookup table
$K_{\text{lookup\_table}}(X_{ac}, X_{ca})$: The stiffness lookup table

The control scheme is illustrated as follows. First, an arbitrary force trajectory is defined by the user to generate the force profile. Second, optimal control is used to find the corresponding trajectories of X_{ac} and X_{ca} that minimize the cost function. Once the position trajectory is generated, two independent position proportional-derivative (PD) controllers are used to control the two actuators. The control flow is shown in Fig. 7, in which the force profile regarding the displacement of X_{ac} and the deflection of X_{ca} by Eqs. 4 and 6 is stored as Fig. 8e. With the lookup table, the optimal force command can be easily approximated. Those points are calculated. The cost and the point with the minimum cost are the optimal results for the next displacement of X_{ac} and deflection of X_{ca}. The major advantage of this algorithm is that it computes quickly and is easily implemented, since it does not need a complicated nonlinear optimal control algorithm.

To verify the proposed method, an upper-extremity exoskeleton system based on the proposed CCEA actuator is adopted, as shown in Fig. 9. To satisfy individual needs of the elbow exoskeleton, a level arm with a forearm holder and an upper-arm holder is designed to move with a subject's forearm and arm. To track the position reference generated in optimal control, a simple position PD controller is used to control the deflection of X_{ca} and the displacement of X_{ac}.

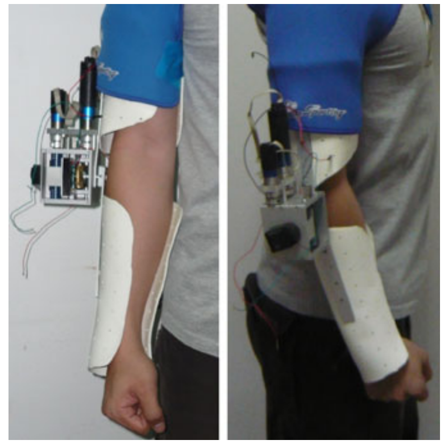

Fig. 9 CCEA exoskeleton for a human elbow

The proportional gain is 120, the derivative gain is 10, and the variable fed into the PID loop is the encoder counts. Finally, a simple experiment is conducted to demonstrate the performance of the force and stiffness control of the CCEA, in which the output link is fixed, the force reference command is given, and the trajectories of the actuators and the force generated by CCEA are collected to illustrate the performance of the shortest distance algorithm.

5 Results and Discussion

5.1 CCEA Potential Energy, Force, and Stiffness

The stiffness, force, and potential energy of single and antagonist four-bar linkage are shown in Fig. 8. The system demonstrates different mechanical properties efficiently by adjusting X_{ac}, especially, near zero mechanical stiffness, which is rare compared to state-of-art designs. The CCEA with various mechanical properties can regulate safety and performance in various tasks. Briefly, the variable stiffness actuators can be achieved by the nonlinear displacement mechanism with a constant stiffness structure [11–17] or a nonlinear stiffness structure with constant displacement [10]. The CCEA is a nonlinear displacement mechanism with a constant stiffness structure, nonlinear displacement is achieved with four-bar linkage, and adjusting the preload of the constant

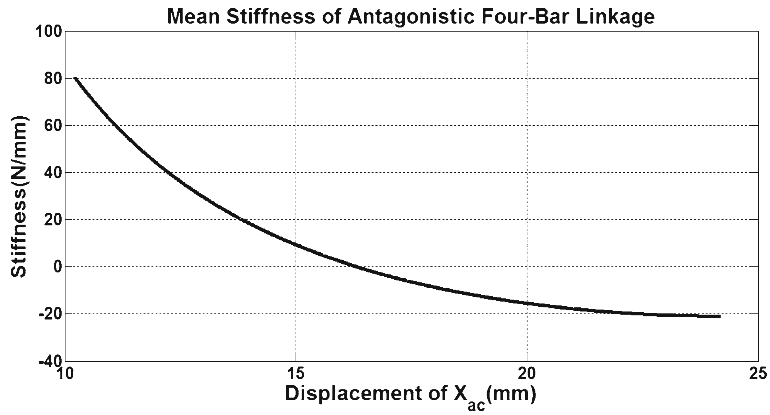

Fig. 10 Average stiffness of antagonistic four-bar linkages

spring can change the natural stiffness curve of the CCEA. Compared to previous compliant or stiff actuators, an actuator using the proposed CCEA approach not only exhibits the desired ranges of intrinsic output impedance but also performs adjustable force profiles corresponding to the deviation between human motions and the set positions of the system. Moreover, the output stiffness can be controlled by using an incomparable, prompt, and relatively small adjusting actuator while delivering output force using coupled parallel elasticity.

The result for the average stiffness with different displacement of X_{ac} is shown in Fig. 10. The figure reveals an interesting result: The stiffness decreases as X_{ac} increases and ranges from 80.703 N/mm to −21.009 N/mm. When the displacement of X_{ac} is 16.327 (the angle of β is approximate to 70.678 degrees), the average stiffness is approximately zero. The curve is approximate to Eq. 11.

$$k_1 = k_g \left(0.0109 X_{ac}^2 - 0.4774 X_{ac} + 4.8861\right), \; k_g = 62 \tag{11}$$

By observing the potential energy of the antagonistic four-bar linkage, when the value of X_{ac} is larger than 16.327, the deflection of X_{ca} makes the CCEA store energy. In contrast, when the value of X_{ac} is smaller than 16.327, the deflection of X_{ca} makes the CCEA release energy. The additional property of native stiffness may have another unknown useful benefit, but this paper mainly considers variable stiffness from zero to a suitable value, such as 80 N/mm. Finally, this property can be achieved easily through the antagonistic mechanism.

5.2 Results for Optimal Control in a Simple Model of Variable Stiffness Actuation

The results for the optimal stiffness and equilibrium position for variable stiffness actuation are shown in Fig. 11. The aim of the cost function J_0 is to minimize the two norms of the control input, displacement, velocity, and tracking error. The result for J_0 shows the change rate of the stiffness and velocity of the equilibrium point are lower than J_1 and J_2, especially for J_2. From the high to low value, the average stiffness is J_0, J_1, and J_2. This implies that the average stiffness increases as the frequency increases as the cost function includes the control input (u_1 &u_2), displacement of the equilibrium point (z_1), velocity of the equilibrium point (z_2), stiffness (z_3), and stiffness change rate (z_4). J_1 minimizes the two norms of the control input, displacement, and tracking error. Because minimizing the two norms of velocity is similar to minimizing kinetic energy, which is part of the input energy, the result for J_1 is similar to that for J_0. However, J_2 minimizes only the two norms of displacement and tracking error. The result for J_2 is much different from that for J_1 and J_0. To observe the results of three cost functions, the relationship between the stiffness

Fig. 11 Optimal control result of three objective functions with force trajectory of 10 sin(2πt) in a simple model of variable stiffness actuation. **a** Result for optimal control J_0. **b** Result for optimal control J_1. **c** Result for optimal Q4 control J_2

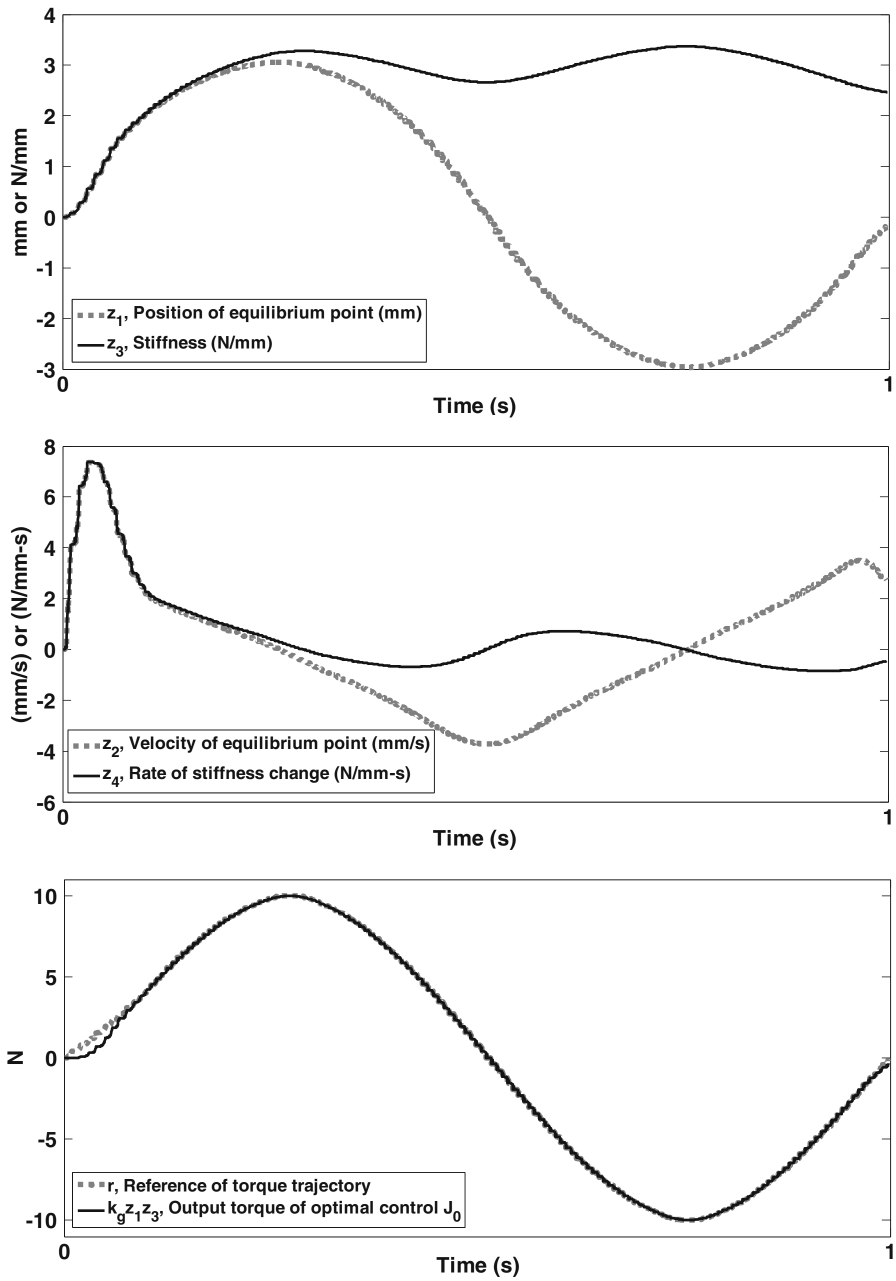

(a)

and the equilibrium point can approximated as follows:

$$k_g z_3 \approx |z_1|\,,\ z_3 > 0 \tag{12}$$

$$F = k_g z_3 z_1 \approx k_g z_3^2 \tag{13}$$

$$z_3 \approx \sqrt{F/k_g}. \tag{14}$$

The optimal results happened as the stiffness is proportional to the equilibrium point. As described, the result shows some properties are

Q4 **Fig. 11** (continued)

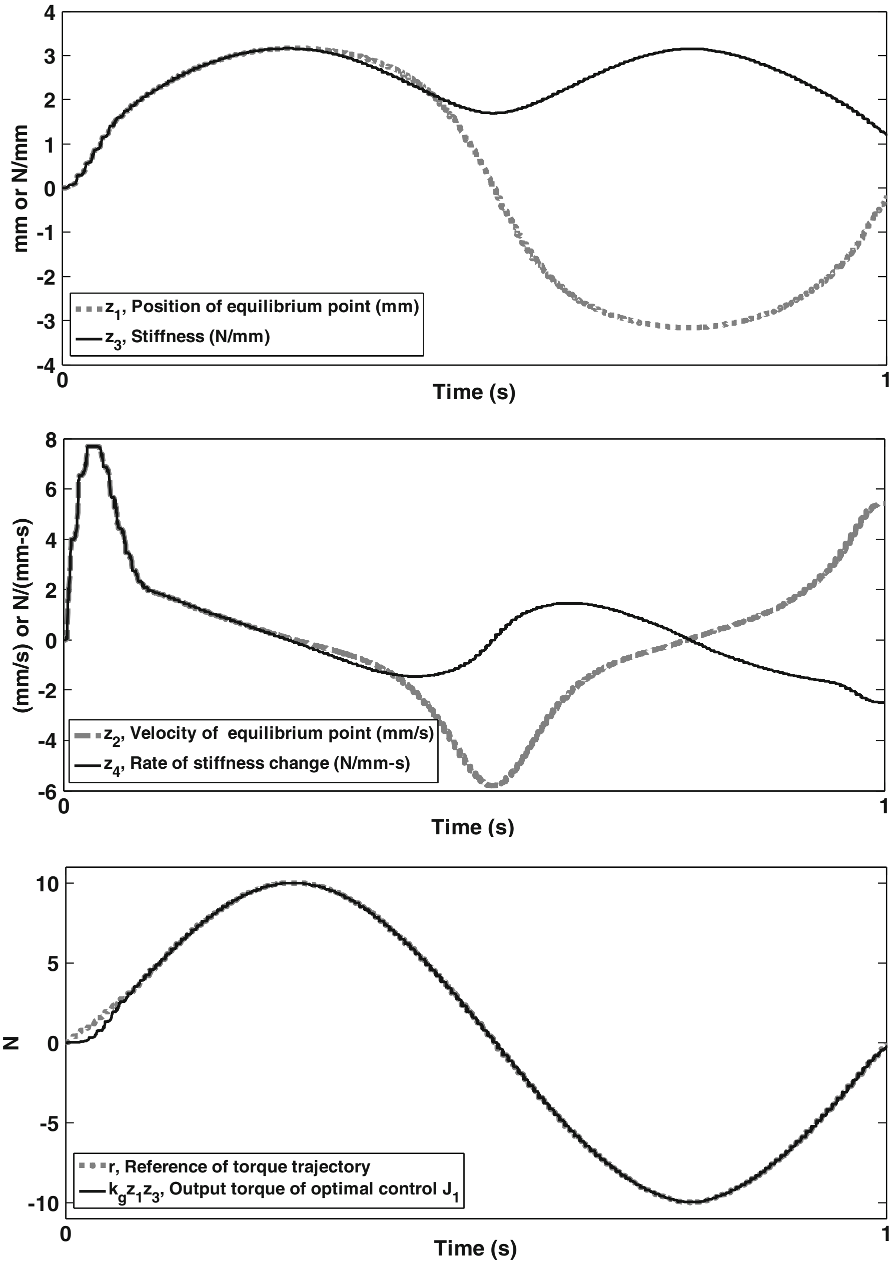

(b)

similar to human muscle. According to Farahat and Herr [37], the human muscle force model is modeled such that the muscle force is bilinear in the equilibrium position and the muscle activation level, and the stiffness is proportional to the muscle activation level. In two opposite types of movements, the muscle activation will increase. One is the fixed output angle with slowly increasing muscle force, and the other is rapid free motion without a fixed output angle. The first condition is the muscle performance in low frequency, and the second is in high frequency. In the first condition, Q4 **Fig. 11** (continued)

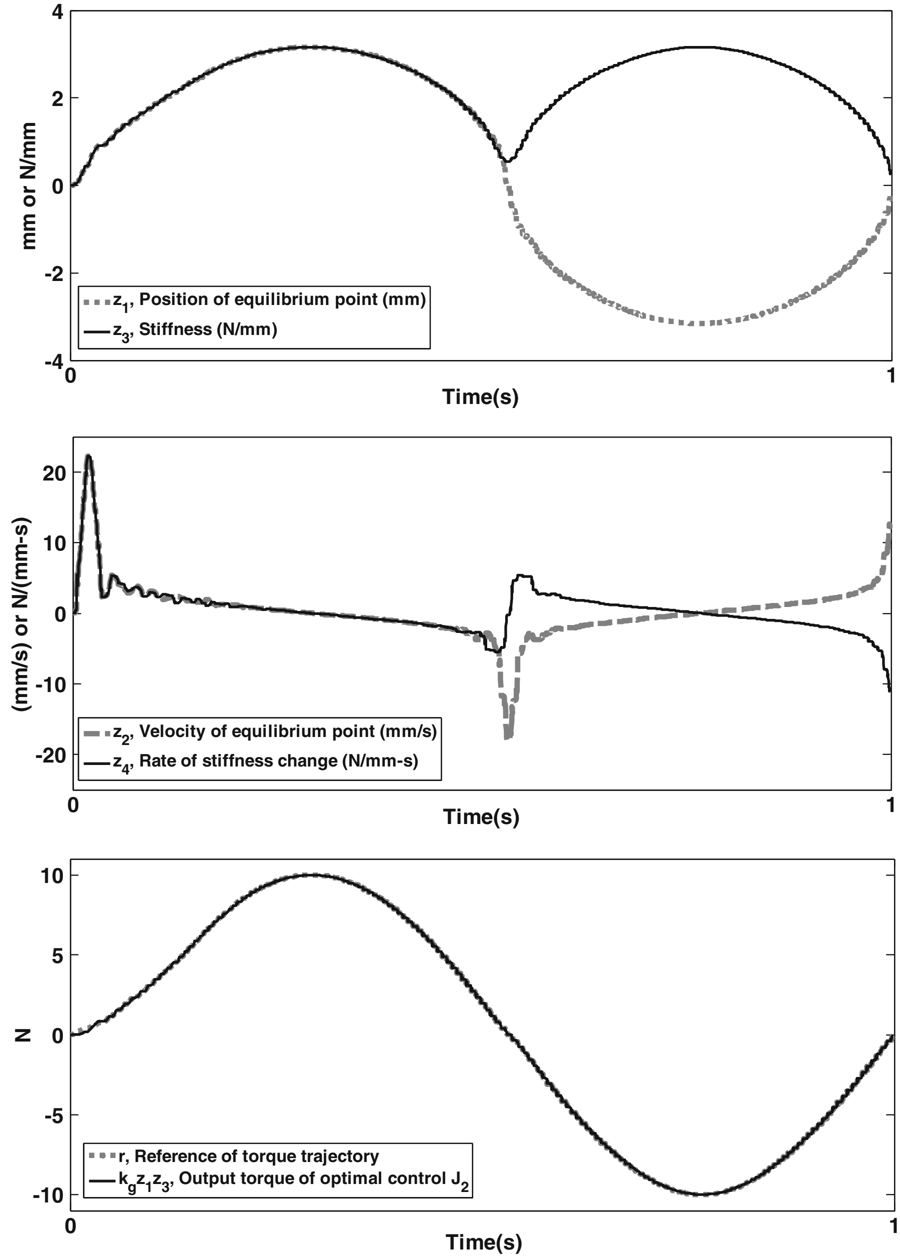

(c)

the stiffness increases as the force increases. In the second condition, the stiffness increases as the frequency increases. Those properties are similar to the results for optimal variable stiffness control. In addition, the relationship of stiffness, force, and motion frequency is possibly generated according to the minimum energy consumed in nature. Although the model is only a simple CCEA model, the property of system with coupled stiffness and equilibrium position is similar to the system with independent stiffness and equilibrium position. They will have similar results in minimizing the

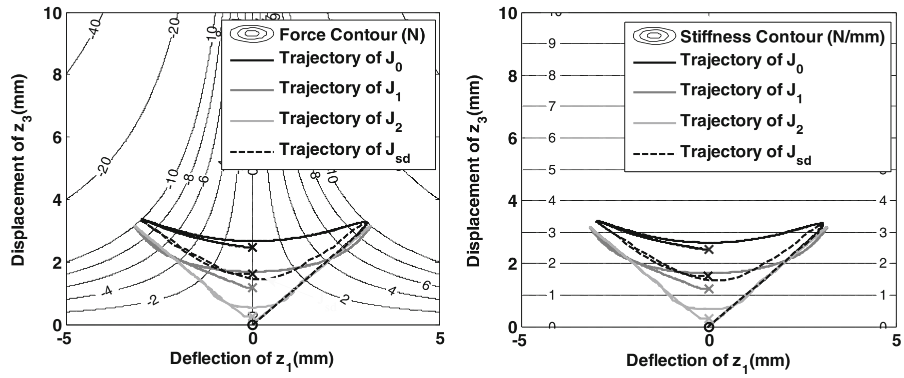

Fig. 12 Force and stiffness trajectories of different objective functions in a simple variable stiffness actuation

energy of the control input, state variables, and tracking error.

5.3 Simulation Results for Force and Stiffness Control in the CCEA

The results for the simple variable stiffness actuation are shown in Fig. 12, and the results for the CCEA force and stiffness control are shown in Fig. 13. The different cost functions are compared in Fig. 12, which reveals the trajectory of J_2 is similar to the trajectory of J_{sd} and the optimal method of J_{sd} is easier and faster than the optimal control method of J_2.

The results for the force and stiffness trajectory in the CCEA are shown in Fig. 13. It reveals the results for a coupled mechanism, such as the CCEA, and an independent mechanism, such as a simple various stiffness mechanism, are similar. The mechanisms have similar force and stiffness trajectories, although they have different mechanisms.

5.4 Experimental Results for Assistive Control

The control result is shown in Fig. 14, and the trajectories of X_{ac} and X_{ca} are shown in Fig. 15. The solid line is the force command, the dashed line is the measured force from the potentiometer and encoder of the CCEA, and the dotted line is the tracking error. The errors come mainly from the output backlash of the worm and the worm gear, the steady state error of the PD position control, the torque error from the cross term of the actuator position tracking error, and the truncation error from the force lookup table. The error from backlash can be induced by considering the backlash in the dynamic equation. The state error

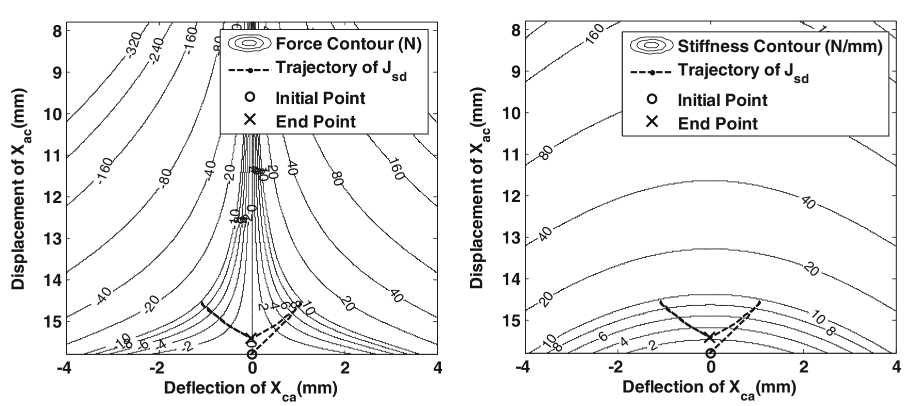

Q4 **Fig. 13** Force and stiffness trajectories of Jsd in the CCEA

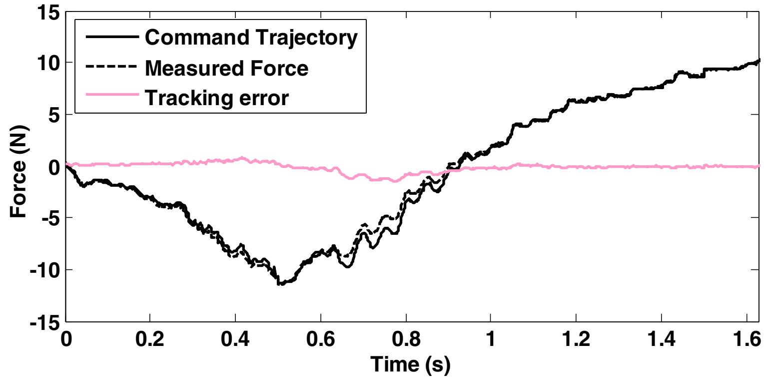

Fig. 14 Experimental results for the force and stiffness control in the CCEA

of the PD control and the torque error from the cross term from the actuation position tracking error can be reduced by choosing a suitable PD gain or applying some nonlinear control, such as a sliding mode control to minimize the position error in each actuator. The truncation error can be reduced with a more precise lookup table, but it will increase the computation time. The experimental results show slight tracking errors. However, these errors are relatively small. Finally, the proposed system provides a gentle way to accomplish various tasks, and the various stiffness and force controls are achieved by the shortest distance between the current point and the next point. The benefits are shorter computation time and the ease of implementing any type of various stiffness mechanism. The system does not need to know the precise mechanical modes of the various stiffness mechanisms.

6 Conclusions

In this paper, a novel CCEA approach, a general optimal control for variable stiffness control, and the shortest path control for variable stiffness and force controls in the CCEA have been proposed to give a robot system an intrinsically programmable stiffness capacity. As a possible design of the proposed actuation approach, a CCEA design with adjustable characteristics according to an applied output force and an input force has also been designed to provide a favorable solution via a novel torque transmission mechanism with a pair of four-bar linkages. The proposed CCEA system possesses intrinsic advantages of being adjustable to compromise safety with performance and providing flexibility for an individual user with good performance. In addition, the optimal control and the shortest distance control are used to choose

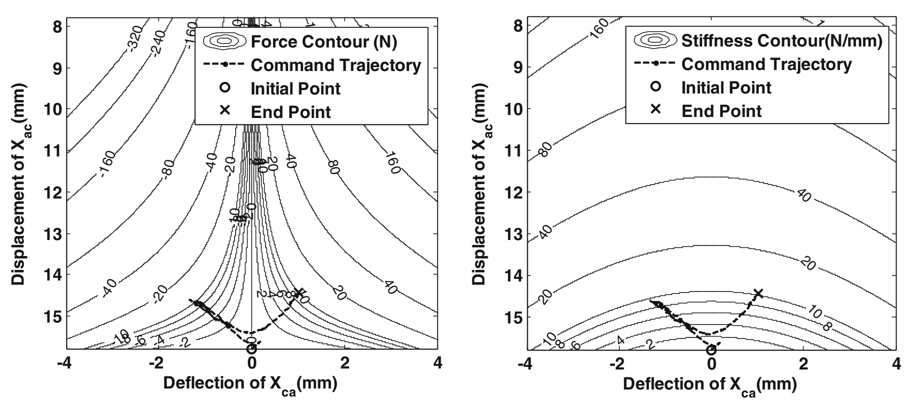

Fig. 15 Command trajectory on force and stiffness contour

the optimal stiffness and force trajectories. The conclusions are the shortest distance control has similar results as the optimal control method and can be implemented and extended very easily to any type of various stiffness mechanism. In the future, estimating human muscle stiffness and using human impedance to change the stiffness for the best performance and safety should be researched and addressed. Considering the repeatability in the application of assistive humans or rehabilitation, the repeatability analysis of this CCEA is also important. Future work will also conduct the repeatability test in rehabilitation and assistive exercise in a clinic. In summary, the proposed CCEA approach with the proposed shortest distance control are good choices for providing future human-machine systems with an intrinsic way to deal with different requirements and to help individuals with weak muscle ability.

Acknowledgements This work was partially supported by the National Science Council of the R.O.C. under grants NSC 100-2221-E-002-127-MY3, NSC 100-2221-E-002-077-MY3.

References

1. Edsinger, A.L.: Robot Manipulation in Human Environments. Doctoral dissertation, Massachusetts Institute of Technology (2007) Q6
2. Taix, M., Flavigne, D., Ferre, E.: Human interaction with motion planning algorithm. J. Intell. Robot. Syst. **67**(3–4), 285–306 (2012)
3. De Luca, A., Albu-Schaffer, A., Haddadin, S., Hirzinger, G.: Collision detection and safe reaction with the DLR-III Lightweight manipulator arm. In: IEEE International Conference on Intelligent Robots and Systems, pp. 1623–1630. Beijing, China (2006) Q6
4. Bonilla, I., Reyes, F., Mendoza, M., Gonzalez-Galvan, E.J.: A dynamic-compensation approach to impedance control of robot manipulators. J. Intell. Robot. Syst. **63**(1), 51–73 (2011)
5. Correa, M., Hermosilla, G., Verschae, R., Ruiz-del-Solar, J.: Human detection and identification by robots using thermal and visual information in domestic environments. J. Intell. Robot. Syst. **66**(1–2), 223–243 (2012)
6. Edsinger-Gonzales, A., Weber, J.: Domo: A force sensing humanoid robot for manipulation research. In: Proceedings of the 4th IEEE-RAS International Conference on Humanoid Robots, pp. 273–291. Santa Monica, CA, USA (2004) Q6
7. Lauria, M., Legault, M.-A., Lavoie, M.-A., Michaud, F.: High performance differential elastic actuator for robotic interaction tasks. In: AAAI Spring Symposium, pp. 39–41. Stanford University Press, Stanford (2007) Q7
8. Sensinger, J.W., Weir, R.F.: Design and analysis of a non-backdrivable series elastic actuator. In: IEEE International Conference on Rehabilitation Robotics, pp. 390–393. University of Chicago Press, Chicago (2005) Q7
9. Torres-Jara, E., Banks, J.: A simple and scalable force actuator. In: 35th International Symposium on Robotics, Paris-Nord Villepinte, France (2004) Q6
10. Robinson, D.W.: Design and analysis of series elasticity in closed-loop actuator force control. Doctoral dissertation, Massachusetts Institute of Technology (2000) Q6
11. Kyoungchul, K., Joonbum, B., Tomizuka, M.: Control of rotary series elastic actuator for ideal force-mode actuation in human-robot interaction applications. IEEE/ASME Trans. Mech. **14**(1), 105–118 (2009)
12. Huang, T.H., Kuan, J.Y., Huang, H.P.: Design of a new variable stiffness actuator and application for assistive exercise control. In: Proceedings of 2011 IEEE/RSJ International Conference on Intelligent Robots and Systems (IROS), pp. 372–377. San Francisco Press, San Francisco (2011) Q7
13. Kyoungchul, K., Joonbum, B., Tomizuka, M.: A compact rotary Series elastic actuator for human assistive systems. IEEE/ASME Trans. Mech. **17**(2), 288–297 (2012)
14. Bigge, B., Harvey, I.R.: Programmable springs: developing actuators with programmable compliance for autonomous robots. Robot. Auton. Syst. 55(9), 728–734 (2007)
15. Hurst, J.W., Chestnutt, J.E., Rizzi, A.A.: An actuator with mechanically adjustable series compliance. In: Tech. Rep. CMU-RI-TR-04-24, Robotics Institute. Carnegie Mellon University, Pittsburgh (2004) Q7
16. Wolf, S., Hirzinger, G.: A new variable stiffness design: matching requirements of the next robot generation. In: IEEE International Conference on Robotics and Automation, pp. 1741–1746. Pasadena, California, USA (2008) Q7
17. Migliore, S.A., Brown, E.A., DeWeerth, S.P.: Novel nonlinear elastic actuators for passively controlling robotic joint compliance. J. Mech. Design **129**(4), 406–412 (2007)
18. Park, J.-J., Kim, B.-S., Song, J.-B., Kim, H.-S.: Safe link mechanism based on nonlinear stiffness for collision safety. Mech. Mach. Theory **43**(10), 1332–1348 (2007)
19. Park, J.-J., Song, J.-B., Kim, H.-S.: Safe joint mechanism based on passive compliance for collision safety. In: Recent Progress in Robotics: Viable Robotic Service to Human. pp. 49–61. Springer, Heidelberg (2008) Q7
20. Schiavi, R., Grioli, G., Sen, S., Bicchi, A.: VSA-II: a novel prototype of variable stiffness actuator for safe and performing robots interacting with humans. In: IEEE International Conference on Robotics and Automation, pp. 2171–2176. Pasadena, California, USA (2008) Q7
21. Albu-Schaffer, A., Eiberger, O., Grebenstein, M., Haddadin, S., Ott, C., Wimbock, T., Wolf, S., Hirzinger, G.: Soft robotics. IEEE Robot. Autom. Mag. **15**(3), 20–30 (2008)

22. Van Ham, R., Vanderborght, B., Van Damme, M., Verrelst, B., Lefeber, D.: MACCEPA, the mechanically adjustable compliance and controllable equilibrium position actuator: design and implementation in a biped robot. Robot. Auton. Syst. **55**(10), 761–768 (2007)
23. Lan, N., Crago, P.: Optimal control of antagonistic muscle stiffness during voluntary movements. Biol. Cybern. **71**(2), 123–135 (1994)
24. Menegaldo, L.L., Fleury, A.d.T., Weber, H.I.: A 'cheap' optimal control approach to estimate muscle forces in musculoskeletal systems. J. Biomech. **39**(10), 1787–1795 (2006)
25. Ning, L., Crago, P.E.: Optimal control of muscle stiffnesses for FNS induced arm movements. In: Proceedings of the Annual International Conference of the IEEE Engineering in Medicine and Biology Society, pp. 920–921. Orlando, Florida, USA (1991) Q7
26. Blaya, J.A., Herr, H.: Adaptive control of a variable-impedance ankle-foot orthosis to assist drop-foot gait. IEEE T. Neural Syst. Rehabil. Eng. **12**(1), 24–31 (2004) Q8
27. Hollander, K.W., Sugar, T.G., Herring, D.E.: Adjustable robotic tendon using a 'Jack Spring'/spl trade. In: Sugar, T.G. (ed.) International Conference on Rehabilitation Robotics, pp. 113–118. University of Chicago Press, Chicago (2005) Q7
28. Walker, D.S., Niemeyer, G.: Examining the benefits of variable impedance actuation. In: 2010 IEEE/RSJ International Conference on Intelligent Robots and Systems (IROS), pp. 4855–4861. Taipei, Taiwan, ROC (2010) Q7
29. Kolacinski, R.M., Quinn, R.D.: A novel biomimetic actuator system. Robot. Auton. Syst. **25**(1–2), 1–18 (1998)
30. Hurst, J.W., Chestnutt, J.E., Rizzi, A.A.: The actuator with mechanically adjustable series compliance. IEEE T. Robot. **26**(4), 597–606 (2010) Q8
31. Visser, L.C., Carloni, R., Stramigioli, S.: Energy-efficient variable stiffness actuators. IEEE T. Robot. **27**(5), 865–875 (2011) Q8
32. Leavitt, J., Jabbari, F., Boborw, J.E.: Optimal control and performance of variable stiffness devices for structural control. In: 2005 American Control Conference, pp. 2499–2504. Portland, OR, USA (2005) Q7
33. Braun, D., Howard, M., Vijayakumar, S.: Optimal variable stiffness control: formulation and application to explosive movement tasks. Auton. Robot. **33**(3), 237–253 (2012)
34. Hadiyanto, H., Esveld, D.C., Boom, R.M., van Straten, G., van Boxtel, A.J.B.: Control vector parameterization with sensitivity based refinement applied to baking optimization. Food Bioprod. Process. **86**(2), 130–141 (2008)
35. Coleman, T., Branch, M.A., Grace, A.: Optimization Toolbox for Use with MATLAB User's Guide Version 2. The MathWorks, Inc. (1998) Q6
36. Hayet, J.B.: Shortest length paths for a differential drive robot keeping a set of landmarks in sight. J. Intell. Robot. Syst. **66**(1–2), 57–74 (2012)
37. Farahat, W.A., Herr, H.M.: Optimal workloop energetics of muscle-actuated systems: an impedance matching view. PLoS Comput. Biol. **6**(6), e1000795 (2010)